

Self-consistent optical potential for atoms in solids at intermediate and high energies

T. Fujikawa and K. Hatada

Graduate School for Science, Chiba University, Inage, Chiba 263-8522, Japan

L. Hedin

Department of Theoretical Physics, Lund University, Sölvegatan 14A, S-223 62 Lund, Sweden

(Received 8 February 2000)

We develop an approximation for the optical potential in a solid valid at intermediate and high energies, say, energies from 50 eV and larger. The approximation builds on the GW expression. We separate the random phase approximation polarization propagator in a core electron and a valence electron part, and then have a corresponding separation of the optical potential. For the valence electron optical potential we use a local density approximation because the charge density changes fairly slowly, whereas we use a nonlocal optical potential for the core electron part. We apply this method to electron-Ar and -Kr elastic scattering, and also to electron scattering from atoms in van der Waals solids, semiconductors, and metals. We find satisfactory agreement with the observed results. We also study the importance of using a nonlocal potential for the core part and the sensitivity to a parameter, the average excitation energy. We compare the present results with those calculated by the Hartree-Fock, Dirac-Hara, and Hedin-Lundqvist potentials. The Hedin-Lundqvist potential is rather good for the description of large-angle scattering, whereas none of the local potentials can describe small-angle scattering well.

I. INTRODUCTION

Elastic and inelastic scattering of electrons provides useful information on the atomic structure and properties of bulk solids as well as solid surfaces. Low-energy electron diffraction¹ (LEED) and reflection high-energy diffraction² (RHEED) utilize elastic scattering of a beam of electrons from a surface. Photoelectron diffraction³ and x-ray absorption fine structure⁴ (XAFS) use elastic scattering of photoelectrons excited from a specific deep core level. In the case of extended energy-loss fine structure (EELFS), both inelastic scattering of the probe electrons and elastic scattering of secondary excited photoelectrons play an important role.⁵

It has long been recognized that elastic scattering of electrons is determined by the self-energy for the one-electron Green's function (optical potential) and its associated one-electron damping function,⁶⁻⁸ and explicit discussions have been made for x-ray photoemission spectroscopy (XPS),⁹ extended XAFS (EXAFS),¹⁰ and EELFS.^{11,12}

Consider elastic electron scattering on a neutral atom. The Hartree and exchange potentials are short ranged and decay exponentially while the polarization potential V_{pol} goes as $1/r^4$. In the Born approximation the scattering amplitude is just the Fourier transform of the potential. The long tail of V_{pol} has small large- q components, and thus gives little backscattering. Byron and Joachain¹³ studied elastic electron scattering on atoms (helium and neon) at 400 eV including a (simplified) V_{pol} . They found that V_{pol} was quite important not only for small-angle scattering. Thus it could be important to include core polarization also for solids where the long-ranged tails in the potentials are cut off by screening effects. We have earlier developed a theory for a practical, self-consistent and nonlocal optical potential in a solid¹⁴ and applied it to electron atom scattering [He,¹⁵ Ne, and Ar (Ref. 16)], where good agreement with the experimental results was obtained. Here this theory is extended in particular as

regards the effects of the ion core polarization potential in solid-state problems.

To calculate elastic scattering from atoms in a solid, a muffin-tin-type potential is constructed from which a set of phase shifts is obtained. The construction of an effective one-electron potential requires knowledge of the electronic charge density and a theory for calculating the exchange-correlation potential. A simplified local exchange potential was proposed by Slater.¹⁷ For electrons with a uniform density ρ in a large box, the Hartree-Fock exchange contribution can be found analytically. Slater averaged this exchange contribution for electrons below the Fermi surface, and assumed that the exchange potential in a solid could be approximated by a local potential whose value at point \mathbf{r} was set equal to this electron-gas-averaged exchange taken at the solid-state density $\rho(\mathbf{r})$, which gives the Slater exchange potential

$$V_{ex}(\mathbf{r}) \sim -(3/2)(3\rho(\mathbf{r})/\pi)^{1/3}. \quad (1.1)$$

This potential is widely used, not only for electrons below the Fermi level, but also for scattering problems, where it is basically incorrect. Thus for high energies exchange scattering can be neglected, whereas the Slater exchange potential still has an influence. Another even more widely used variant of Slater's intuitive ideas is the X_α potential. Here the Slater potential is multiplied by an empirical parameter α , $V_{X_\alpha} = \alpha V_{ex}$, where α often is taken as $2/3$.¹⁸ The $X_{2/3}$ potential is the same as the exchange-only Kohn-Sham ground-state potential²² and as the Dirac potential.¹⁹ Sometimes it is called the Kohn-Sham-Gáspar potential since Gáspar¹⁸ long ago found that, for the Cu atom, it gave better agreement with the pure Hartree-Fock potential than did the Slater one. For scattering problems the exchange potential before averaging is more motivated. This potential is local and energy dependent, and it was shown by Hara²⁰ to be successful for

electron scattering from atoms and molecules. It is often called the ‘‘Dirac-Hara’’ potential even though there is little reason to attach the name Dirac here.

These methods employ the Hartree-Fock approximation for a uniform electron gas. One expects that going beyond the Hartree-Fock approximation to the electron self-energy within a local density approximation should give an improved scattering potential. Hedin and Lundqvist²¹ (HL) suggested a scheme based on the Sham-Kohn theory,²² where the electron gas self-energy $\Sigma_0(q, \varepsilon(q))$ is used with a density-dependent momentum $q(\mathbf{r})$. Following Hedin and Lundqvist²¹ Lee and Beni applied such a potential to electron scattering from atoms in the intermediate-energy region, using the plasmon pole approximation to the GW self-energy, and showed that this potential gives an excellent description of the EXAFS data for Br₂, GeCl₄, and Ge.²³ Several authors have compared these potentials for LEED (Refs. 24–26) and XAFS calculations.^{23,27–30} In principle the Hedin-Lundqvist potential should give the best result among those methods described above; however, the results are not so clear-cut; sometimes we can find a value α in the X_α potential which gives a better result than the Hedin-Lundqvist potential.²⁶

We have developed a method to calculate a self-consistent nonlocal energy-dependent optical potential based on Hedin’s GW approximation.^{7,8} Previous short communications described an outline of the theory,¹⁴ and applied it to electron-atom scattering^{15,16} where we found good agreement between the calculated and experimental results. We also studied the effect of self-consistency and the sensitivity to an average excitation energy. In this work we give a detailed description of the method, and compare the elastic electron scattering cross sections calculated from the present nonlocal optical potential with those from the Hartree-Fock (HF) approximation and from different local density approximations. Results are shown both for scattering from free atoms and from atoms in a solid.

II. BASIC THEORY

The optical potential for the target state $|0\rangle$ is given to lowest nontrivial order in a Van Hove–type expansion¹¹

$$\Sigma_0(E) = \sum_{n(\neq 0)} \frac{\langle 0|V|n\rangle\langle n|V|0\rangle}{E - E_n - h - \Sigma_0(E - \omega_n) + i\eta}, \quad (2.1)$$

where $E = E_0 + \varepsilon_k$, $\omega_n = E_n - E_0$ (E_n and E_0 are the energy eigenvalues of the target Hamiltonian H_s , $H_s|n\rangle = E_n|n\rangle$ and $H_s|0\rangle = E_0|0\rangle$), and V is the interaction potential between the scattering electron and the target:

$$V = \sum_{\mathbf{p}\mathbf{q}} \left[\sum_{lm} c_l^\dagger c_m \langle \mathbf{p}l || \mathbf{q}m \rangle + \langle \mathbf{p}l | V_{en} | \mathbf{q} \rangle \right] c_{\mathbf{p}}^\dagger c_{\mathbf{q}}. \quad (2.2)$$

Here V_{en} is the Coulomb interaction between the scattering electron and the positive nuclei in the target, and $\langle \mathbf{p}l || \mathbf{q}m \rangle$ an antisymmetrized Coulomb matrix element.¹¹ The one-electron states of the scattering electron are denoted by \mathbf{p} and \mathbf{q} , and those of electrons in the target by l and m . The interaction V_{en} gives no contribution to the inelastic matrix elements $\langle 0|V|n\rangle$ ($n \neq 0$). When we consider core excitation processes as in XAFS and XPS spectra, the core hole effects

are included only in the one-electron scattering Hamiltonian $h = T_e + \langle 0|V|0\rangle$, where T_e is kinetic energy operator; we can handle the core hole optical potential in the same way as the ground-state optical potential except for some minor differences.¹² Furthermore, we have shown that the optical potential given by Eq. (2.1) is roughly equivalent to the self-energy in the GW approximation,¹¹ so that we will develop a practical method to calculate the atomic optical potential in solids and surfaces based on the GW approximation.

Detailed discussions of the crystal potential have been given long ago by Hedin.^{7,8} As shown below, both the polarization propagator P and one-electron Green’s function G can be split into core and valence parts. The core polarization is assumed to be much smaller than the valence polarization. We thus have an expansion in powers of P^c for the self-energy (optical potential), which is shown in Ref. 8, p. 129, where the following expression for the self-energy (optical potential) is given:

$$\Sigma_0 = G^v W^v + V_{ex}^c + G^v W^v P^c W^v + \dots \quad (2.3)$$

Here $G^v W^v$ is the self-energy from the valence electrons, while V_{ex}^c is the bare exchange and $G^v W^v P^c W^v$ the screened polarization potential from the ion cores. The precise definitions of these quantities are given below.

The next question to consider is the effect of screening in the core-polarization term. For a free atom the screening is small, and we have to a good approximation $G^v v P^c v$, where v is the bare Coulomb potential. For long distances from the ion core it further reduces to the well-known local potential $-\alpha e^2/r^4$, where α is the dipole polarizability.⁷ In a solid we expect from simple physical reasons that for long distances we should have a statically screened polarization potential $G^v W^v(0) P^c W^v(0)$. Since an r^{-4} potential already is very weak, the additional screening should make it negligible outside the Wigner-Seitz cell of the ion under consideration. Inside the Wigner-Seitz cell, on the other hand, we do not expect much screening to take place due to the cost in kinetic energy to localize the screening charge.

The full random phase approximation (RPA) polarization propagator is⁸

$$P(\mathbf{r}, \mathbf{r}'; \omega) = - \sum_k^{unocc} \sum_l^{occ} \frac{2(\varepsilon_k - \varepsilon_l)}{(\varepsilon_k - \varepsilon_l)^2 - \omega^2} f_{kl}(\mathbf{r}) f_{kl}^*(\mathbf{r}'),$$

$$f_{kl}(\mathbf{r}) = \int \psi_k(x) \psi_l^*(x) d\xi. \quad (2.4)$$

Here $x = (\mathbf{r}, \xi)$ includes both space and spin variables. The sum over k runs over unoccupied electron states, while l runs over the occupied core and valence electron states. By splitting the summation over l into core and valence contributions, P can be written as a sum of core and valence parts,

$$P = P^c + P^v. \quad (2.5)$$

Similarly we can split the summation over k in the expression for the one-electron Green’s function,

$$G(x, x'; \omega) = \sum_k^{occ+unocc} \frac{\psi_k(x) \psi_k^*(x')}{\omega - \varepsilon_k}, \quad (2.6)$$

to obtain

$$G = G^c + G^v. \quad (2.7)$$

The symbol $G^v v P^c v$ stands for a convolution in energy space,¹¹ which can be done analytically, giving

$$\begin{aligned} [G^v v P^c v](x, x'; \omega) \\ = \sum_k^{unocc} \sum_l^{core} \sum_{k'}^{valence} \frac{v_{kl}(\mathbf{r}) \psi_{k'}(x) \psi_{k'}^*(x') v_{kl}^*(\mathbf{r}')}{\omega - \omega_{kl} - \varepsilon_{k'}}, \end{aligned} \quad (2.8)$$

where $\omega_{kl} = \varepsilon_k - \varepsilon_l$, and

$$v_{kl}(\mathbf{r}) = \int v(\mathbf{r} - \mathbf{r}') \psi_k^*(x') \psi_l(x') dx'$$

The more tightly bound the core level l is, the smaller its contribution to $v_{kl}(\mathbf{r})$ due to the smaller overlap with the unoccupied function k . Thus the outermost core level will give the dominant contributions.

We replace ω_{kl} by a constant Δ , the average excitation energy. This approximation has been very successful in the free atom case.¹³ We define a function $A(\mathbf{r}, \mathbf{r}')$,

$$\begin{aligned} A(\mathbf{r}, \mathbf{r}') &= \sum_k^{unocc} \sum_l^{core} v_{kl}(\mathbf{r}) v_{kl}^*(\mathbf{r}') \\ &= \int v(\mathbf{r} - \mathbf{r}_1) v(\mathbf{r}' - \mathbf{r}_2) [\delta(x_1 - x_2) - \rho(x_1, x_2)] \\ &\quad \times \rho^c(x_2, x_1) dx_1 dx_2, \end{aligned} \quad (2.9)$$

where the last equality follows by closure, and ρ and ρ^c are the one-electron density matrices for all electrons and for core electrons, respectively. With $\omega_{kl} = \Delta$ we then have

$$\begin{aligned} V^{pol}(x, x'; \omega) &= [G^v v P^c v](x, x'; \omega) \\ &= A(\mathbf{r}, \mathbf{r}') G^v(x, x'; \omega - \Delta). \end{aligned} \quad (2.10)$$

With the use of closure we avoid the summation over the unoccupied states. Still the density matrix $\rho(x_1, x_2)$ contains a sum over the occupied Bloch functions. We will here take a simplified approach and represent the sum over Bloch functions in each atomic cell α by a sum over localized functions $R_n^\alpha Y_{lm}$. This is well motivated for rare gas solids, but a more serious approximation for, say, metals. In a more accurate treatment one could consider representing the Bloch functions with muffin-tin orbitals, but this would mean an integration in k space, which would substantially increase the computational work.

If \mathbf{r} is in cell α and the core function l is in a neighboring cell β , then $v_{kl}(\mathbf{r})$ is small and depends on the dipole matrix element between k and l . To lowest order the interatomic contribution to A from the first term in Eq. (2.9) is, on the other hand (taking the core functions as completely localized),

$$\frac{N_c^\beta}{|\mathbf{r} - \mathbf{R}_{\beta\alpha}| |\mathbf{r}' - \mathbf{R}_{\beta\alpha}|}, \quad (2.11)$$

where N_c^β is the total number of core electrons in cell β , which is a large contribution that does not contain any dipole

matrix element. To lowest order the second term in Eq. (2.9), however, exactly cancels this contribution since $\int \rho(x_1, x_2) \rho^c(x_2, x_1) dx_1 dx_2 = N_c^\beta$ when the integration over x_1 and x_2 is restricted to cell β . We will evaluate the interatomic contributions to A from a multipole expansion using a bare potential $v(\mathbf{r} - \mathbf{r}_1)$. The results are taken as an upper limit to what we can expect to have with a properly screened potential W .

Byron and Joachain¹³ simplified the expression for the core-polarization potential in Eq. (2.10), and were able to obtain an explicit local approximation. They also approximated the exchange potential by taking the electron gas expression with the local electron density. These approximations for the optical potential gave quite good results for electron-atom scattering.¹³

It is not easy to assess the accuracy of the many different approximations made by Byron and Joachain,¹³ and their approximations are further difficult to generalize to the solid-state case. Instead we prefer to actually evaluate the nonlocal expressions for both the exchange and polarization potentials from the ion cores.

III. ATOMIC OPTICAL POTENTIALS IN SOLIDS

When one studies electron spectroscopies such as LEED and XAFS, the elastic scattering from each atomic site is a crucial physical process. It is therefore important to separate the total effective one-electron potential V_{cryst} into atomic scattering potentials v_α centered at sites α . The v_α are usually spherically averaged to simplify the formulas. The one-electron Green's function can then be represented by a T -matrix expansion in terms of a homogeneous medium Green's function $g_0 = (\varepsilon_p - T_e - \Delta + i\Gamma)^{-1}$. When $\mathbf{r} \in \alpha$ and $\mathbf{r}' \in \beta$, we have to lowest order

$$g(\mathbf{r}, \mathbf{r}') = g_0 + g_0 t_\alpha g_0 + g_0 t_\beta g_0 + \dots, \quad (3.1)$$

where t_α is the T matrix for site α . The damping propagator g_0 is small already at the nearest neighbor distance. The energy-independent term A defined by Eq. (2.9) also decreases with the distance $|\mathbf{r} - \mathbf{r}'|$ [see Eq. (3.25)]. It is hence enough to consider only one-site contributions to $g(\mathbf{r}, \mathbf{r}')$ at higher energies, say, $\varepsilon_p \gtrsim 100$ eV. For a spherically symmetric potential v_α , the Green's function g_α is expanded as

$$g_\alpha(\mathbf{r}, \mathbf{r}') = \sum_L g_l^\alpha(r, r') Y_L(\hat{\mathbf{r}}) Y_L^*(\hat{\mathbf{r}}'),$$

$$g_l^\alpha(r, r') = -2i\bar{p} \exp(i\delta_l^\alpha) R_l^\alpha(\bar{p}r_<) f_l^\alpha(\bar{p}r_>), \quad (3.2)$$

where δ_l^α is the phase shift of the l th partial wave at site α , $\bar{p} = [2(\varepsilon_p - \Delta + i\Gamma)]^{1/2}$, R_l^α and f_l^α are the regular and irregular solutions for the potential v_α , and $r_> = \max(r, r')$ and $r_< = \min(r, r')$. In the large- r limit they have the asymptotic forms

$$R_l^\alpha(\bar{p}r) \sim \sin(\bar{p}r - l\pi/2 + \delta_l^\alpha)/(\bar{p}r), \quad f_l^\alpha(\bar{p}r) \sim h_l(\bar{p}r), \quad (3.3)$$

where h_l is the spherical Hankel function of l th order.

Next we investigate how to calculate the energy-independent term $A(\mathbf{r}, \mathbf{r}')$. In each atomic region α we average the core charge density to obtain a spherically symmetric function

$$d_\alpha^c(r) = \frac{1}{4\pi} \int d\hat{\mathbf{r}} \rho^c(\mathbf{r}). \quad (3.4)$$

Though both \mathbf{r} and \mathbf{r}' are in the same atomic region, \mathbf{r}_1 and \mathbf{r}_2 are not necessarily in the same atomic region. From the first term in the large parentheses in Eq. (2.9), we have an intraatomic contribution to $A(\mathbf{r}, \mathbf{r}')$,

$$I_\alpha(\mathbf{r}, \mathbf{r}') = \sum_L \left(\frac{4\pi}{2l+1} \right)^2 I_\alpha(r, r')_l Y_L(\hat{\mathbf{r}}) Y_L^*(\hat{\mathbf{r}}'), \quad (3.5)$$

where both \mathbf{r} and \mathbf{r}' belong to atomic region α , and also $\mathbf{r}_1 (= \mathbf{r}_2)$ is in region α . Here $I_\alpha(r, r')_l$ is

$$I_\alpha(r, r')_l = S_1^l + S_2^l + S_3^l, \quad (3.6)$$

$$S_1^l = (rr')^{-l-1} \int_0^{r<} d_\alpha^c(r_1) r_1^{2l+2} dr_1, \quad (3.7)$$

$$S_2^l = \frac{r_{<}^l}{r_{>}^{l+1}} \int_{r_{<}}^{r_{>}} d_\alpha^c(r_1) r_1 dr_1, \quad (3.8)$$

$$S_3^l = (rr')^l \int_{r_{>}}^{R_\alpha} d_\alpha^c(r_1) r_1^{-2l} dr_1, \quad (3.9)$$

where R_α is the radius of the atomic region α (muffin-tin radius).

In addition to this intraatomic contribution to the first term of Eq. (2.9) we have the interatomic term, where \mathbf{r} and \mathbf{r}' are still in region α , whereas $\mathbf{r}_1 (= \mathbf{r}_2)$ is in region β ($\beta \neq \alpha$). This term is given by

$$\begin{aligned} I_\alpha^\beta(\mathbf{r}, \mathbf{r}') &= \sum_{LL'} \left(\frac{4\pi}{2l'+1} \right)^2 |F_{LL'}(\mathbf{R}_{\beta\alpha})|^2 (rr')^l \langle r^{2l'} \rangle_\beta \\ &\quad \times Y_L(\hat{\mathbf{r}}) Y_L^*(\hat{\mathbf{r}}') \\ &= \sum_L F_L(r, r'; \mathbf{R}_{\beta\alpha}) Y_L(\hat{\mathbf{r}}) Y_L^*(\hat{\mathbf{r}}'), \end{aligned} \quad (3.10)$$

where in terms of Gaunt's integral $G(LL'|L'')$ $\equiv \int Y_L(\hat{\mathbf{r}}) Y_{L'}(\hat{\mathbf{r}}) Y_{L''}^*(\hat{\mathbf{r}}) d\hat{\mathbf{r}}$

$$\begin{aligned} F_{LL'}(\mathbf{R}_{\beta\alpha}) &= \frac{4\pi(-1)^{l'}(2l+2l'-1)!!}{(2l'-1)!!(2l+1)!!R_{\beta\alpha}^{l+l'+1}} \\ &\quad \times G(l+l', m'-m, L|L') Y_{l+l', m'-m}(\hat{\mathbf{R}}_{\beta\alpha}), \end{aligned} \quad (3.11)$$

$$F_L(r, r'; \mathbf{R}_{\beta\alpha}) = \sum_{L'} \left(\frac{4\pi}{2l'+1} \right)^2 |F_{LL'}(\mathbf{R}_{\beta\alpha})|^2 (rr')^l \langle r^{2l'} \rangle_\beta, \quad (3.12)$$

$$\langle r^{2l} \rangle_\beta = \int_0^{R_\beta} d_\beta^c(r) r^{2l+2} dr, \quad (3.13)$$

$$\mathbf{R}_{\beta\alpha} = \mathbf{R}_\beta - \mathbf{R}_\alpha.$$

We note that $\sum_{m'} |F_{LL'}(\mathbf{R}_{\beta\alpha})|^2$ depends on m . To get rid of this difficulty, we use the spherically averaged value of $\sum_{m'} |F_{LL'}(\mathbf{R}_{\beta\alpha})|^2$. Finally we have the averaged expression of F_L in Eq. (3.10) in terms of the Clebsch-Gordan coefficient $\langle l0l'0|l+l'0 \rangle$, which is denoted F_l^0 ,

$$\begin{aligned} F_l^0(r, r'; \mathbf{R}_{\beta\alpha}) &= (rr')^l \sum_{l'} \left\{ \frac{4\pi(2l+2l'-1)!!}{(2l+1)!!(2l'+1)!!R_{\beta\alpha}^{l+l'+1}} \right\}^2 \\ &\quad \times \langle r^{2l'} \rangle_\beta (2l'+1) \langle l'0l0|l+l'0 \rangle^2. \end{aligned} \quad (3.14)$$

Due to the small extension of the core functions, the dominant contribution comes from $l'=0$,

$$F_l^0(r, r'; \mathbf{R}_{\beta\alpha}) = \frac{4\pi}{(2l+1)^2} \frac{(rr')^l}{R_{\beta\alpha}^{2l+2}} N_c^\beta.$$

This is the same result as obtained from averaging over $\hat{\mathbf{R}}_{\beta\alpha}$ in Eq. (2.11).

The second term in the large parentheses in Eq. (2.9) is more difficult to calculate in general. We note that

$$\rho(x_1, x_2) \rho^c(x_2, x_1) = \sum_i^{occ} \sum_j^{core} d_{ij}(x_1) d_{ij}^*(x_2), \quad (3.15)$$

where $d_{ij}(x) = \phi_i(x) \phi_j^*(x)$, and we assume that the core orbital j is localized on site α . We take both \mathbf{r}_1 and \mathbf{r}_2 to be in the same region α . For the occupied states we will not use Bloch functions but instead take a simplified approach and use localized functions $R_n^\alpha Y_{L_n}$. This is well motivated for rare gas solids, but a more serious approximation for say metals.

By spherically averaging $d_{ij}(x)$ at each site α , we can get a simple representation for Eq. (3.15) as

$$\begin{aligned} \rho(x_1, x_2) \rho^c(x_2, x_1) &\sim \sum_m^{core} d_m^\alpha(r_1) d_m^\alpha(r_2) + \sum_m^{core} \sum_{n \neq m}^{occ} d_{mn}^\alpha(r_1) d_{mn}^\alpha(r_2), \end{aligned} \quad (3.16)$$

$$\mathbf{r}_1, \mathbf{r}_2 \in \alpha,$$

where m and n stand for one-electron atomic states $2s$, $2p_+$, $2p_0$, and so on, in atom α , which have the same angular quantum number $L = (l, m)$. The quantity $d_m^\alpha (= d_{mm}^\alpha)$ is the spherically averaged electron density of the m th atomic function at site α , and d_{mn}^α is the cross charge from the m th and n th atomic functions on site α written in terms of the radial parts of the atomic wave functions, $d_{mn}^\alpha(r) = R_m^\alpha(r) R_n^\alpha(r)^*$. As mentioned R_m^α refers to a localized function, which for metals has a fractional occupation number. When we use this simple approximation in Eq. (2.9), the *intraatomic* contribution to A can be written as

$$J_\alpha(r, r') = \sum_m J_m^\alpha(r) J_m^\alpha(r') + \sum_{m \neq n} J_{mn}^\alpha(r) J_{mn}^\alpha(r'), \quad (3.17)$$

with

$$J_m^\alpha(r) = 4\pi \left\{ \frac{1}{r} \int_0^r r_1^2 d_m^\alpha(r_1) dr_1 + \int_r^\infty r_1 d_m^\alpha(r_1) dr_1 \right\}. \quad (3.18)$$

We see that J_α has only a spherically symmetric contribution.

The *interatomic* contribution J_α^β is not difficult to evaluate,

$$J_\alpha^\beta(r, r') = \sum_m^{core} J_m^{\alpha\beta}(r) J_m^{\alpha\beta}(r'), \quad (3.19)$$

where by taking $r_\alpha = r$, $J_m^{\alpha\beta}(r)$ is given as

$$J_m^{\alpha\beta}(r) = \frac{1}{4\pi} \int d\hat{\mathbf{r}}_\alpha \frac{n_m^\beta}{|\mathbf{r}_\alpha - \mathbf{R}_{\beta\alpha}|}, \quad (\alpha \neq \beta). \quad (3.20)$$

Here n_m^β is the number of electrons on site β , and $\mathbf{R}_{\beta\alpha} = \mathbf{R}_\beta - \mathbf{R}_\alpha$. If we evaluate the angular integral in Eq. (3.20), we have

$$J_m^{\alpha\beta}(r) = \frac{n_m^\beta}{|\mathbf{R}_{\beta\alpha}|}, \quad J_\alpha^\beta(r, r') = \frac{N_c^\beta}{|\mathbf{R}_{\beta\alpha}|^2}.$$

Cross terms such as d_{mn}^β give no contribution to $J_m^{\alpha\beta}$ because of the orthogonality between m th and n th shell functions. Therefore $A(\mathbf{r}, \mathbf{r}')$ can be written as

$$A(\mathbf{r}, \mathbf{r}') = \sum_L A(r, r')_l Y_L(\hat{\mathbf{r}}) Y_L^*(\hat{\mathbf{r}}'), \quad (3.21)$$

where A is a sum of one- and two-center terms,

$$A(r, r')_l = A_\alpha(r, r')_l + \sum_{\beta \neq \alpha} A_\alpha^\beta(r, r')_l, \quad (3.22)$$

$$A_\alpha(r, r')_0 = (4\pi)^2 [J_\alpha(r, r')_0 - 4\pi J_\alpha(r, r')_0], \quad (3.23)$$

$$A_\alpha(r, r')_l = \left(\frac{4\pi}{2l+1} \right)^2 I_\alpha(r, r')_l \quad (l \geq 1), \quad (3.24)$$

$$A_\alpha^\beta(r, r')_l = \frac{(4\pi)^2}{3} \left(\frac{l+1}{2l+1} \right) \frac{\langle r^2 \rangle_\beta}{R_{\beta\alpha}^{2l+4}} (rr')^l + \dots \quad (3.25)$$

We find a good convergence for the two-center sum, the second term in Eq. (3.22), when we include the surrounding atoms up to the third shell for the systems considered here.

The optical potential can be given by Eq. (3.26) after the spherical averaging of the potential over $\hat{\mathbf{r}}$ and $\hat{\mathbf{r}}'$ in the same atomic region,

$$V^{pol}(\mathbf{r}, \mathbf{r}'; E_0 + \varepsilon_p) = \sum_L V_l^{pol}(r, r'; \varepsilon_p) Y_L(\hat{\mathbf{r}}) Y_L^*(\hat{\mathbf{r}}'), \quad (3.26)$$

where V_l^{pol} is expressed in terms of $A_{l'}$, $g_{l''}$, and Clebsch-Gordan coefficients,

$$V_l^{pol}(r, r'; \varepsilon_p) = \frac{1}{4\pi} \sum_{l'l''} \frac{(2l'+1)(2l''+1)}{2l+1} \langle l'0l''0|l0 \rangle^2 \times A_{l'}(r, r') g_{l''}^\alpha(r, r'; \bar{p}). \quad (3.27)$$

As demonstrated before it is enough only to include A_0 and A_1 in the expansion Eq. (3.27).¹⁴ We thus obtained an explicit expression for V_l^{pol} ,

$$V_l^{pol}(r, r'; \varepsilon_p) = \frac{1}{4\pi} [A_0(r, r') g_l(r, r'; \bar{p}) + 3A_1(r, r') \tilde{g}_l(r, r'; \bar{p})], \quad (3.28)$$

where \tilde{g}_l is defined by

$$\tilde{g}_l(r, r'; \bar{p}) = \frac{l}{2l+1} g_{l-1}(r, r'; \bar{p}) + \frac{l+1}{2l+1} g_{l+1}(r, r'; \bar{p}). \quad (3.29)$$

Each g_l includes the radial solution for the potential $V_l^{pol}(\varepsilon_p)$ to be determined. Since V_l^{pol} depends on g_l and $g_{l\pm 1}$ we in principle have to solve coupled self-consistent equations.

IV. RESULTS AND DISCUSSION

The total crystal potential V^{cryst} is given by the Hartree potential plus the self-energy Σ_0 in Eq. (2.3). For the potential from the valence electrons, $\Sigma^v = G^v W^v$, we use the Hedin-Lundqvist local approximation,²¹ for V_{ex}^c a proper nonlocal exchange potential (HF), and for $V^{pol} = G^v W^v P^c W^v$ the potential we just have discussed. The core electrons are taken as localized, also the outer core electrons which form valence bands in rare gas crystals. The occupied Bloch functions are replaced by localized functions with occupation numbers which can be fractional, $3s^1 3p^3$ for Si, $3s^1$ for Na, and $3d^{7.4} 4s^{0.6}$ for Fe.

We want to study the scattering properties of this potential. To obtain a sum of potentials centered on different sites (called α or β) we use the muffin-tin approximation. The potential inside the muffin tins is spherically averaged. The average of the potential outside the muffin tins, V_0 (a complex number), is subtracted. In applications to different spectroscopies we need a Green's function $G(E) = [E - T_e - V^{cryst}]^{-1}$. We can then take $[E - T_e - V_0]^{-1}$ as the unperturbed propagator and $(V^{cryst} - V_0)$ as the scattering potential. The handling of a nonlocal potential at the muffin-tin radius causes problems. We have simply put $V(\mathbf{r}, \mathbf{r}') = 0$ when \mathbf{r} or \mathbf{r}' is larger than the muffin-tin radius, and taken the contribution to V_0 as $V(R, R)$, where R is the muffin-tin radius, and V stands for V_{ex}^c or V^{pol} . This potential is denoted by FH, and results obtained with the FH potential are always represented by a full-drawn line in the figures. The FH results are compared with other choices of potentials.

A. Elastic scattering from free Ar and Kr atoms

Several theoretical methods based on local density approximations have been developed to calculate scattering phase shifts^{13,23-30} and used to predict LEED (Refs. 24-26) and XAFS spectra.^{23,27-30} However, factors such as atomic

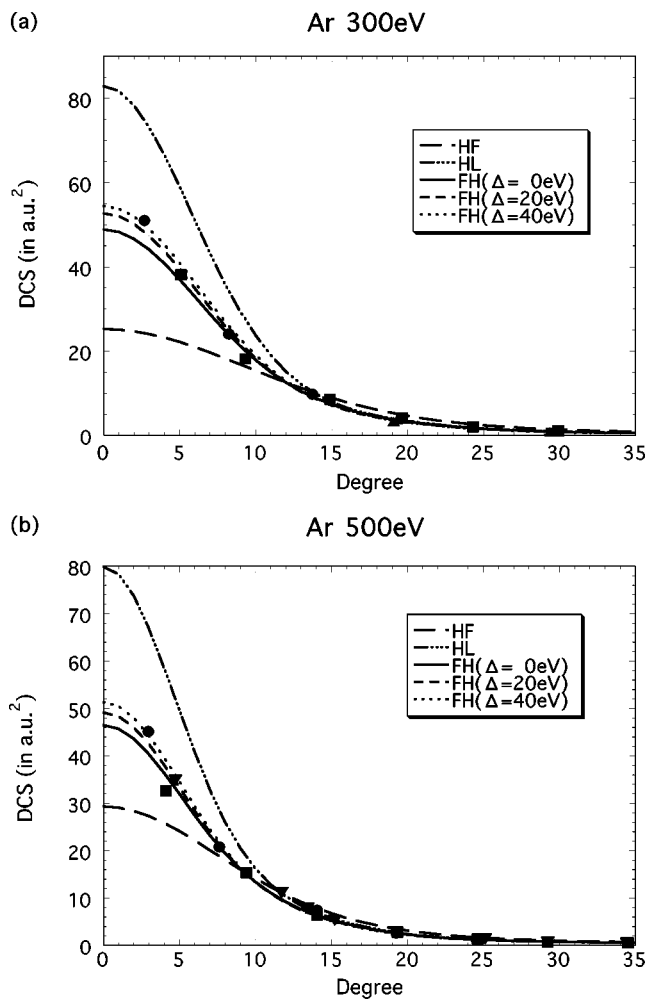


FIG. 1. Differential cross section (DCS) in a.u. as a function of scattering angle for electron elastic scattering from Ar at (a) 300 eV and (b) 500 eV. The solid line shows the result for the present method with $\Delta = 0$ eV, the dashed line with $\Delta = 20$ eV, and the dotted line with $\Delta = 40$ eV. Some experimental results are also shown for comparison. Experimental data \bullet , \blacktriangle , \blacktriangledown , and \blacksquare are from, respectively, Refs. 31–34. The results from the Hartree-Fock and Hedin-Lundqvist potentials are also shown for comparison.

vibrations³⁵ and spherical wave effects³⁶ were not taken into account, and the comparisons are thus uncertain. It is hence of interest instead to compare with results from our method, which has been shown to give satisfactory results for the intermediate-energy region for electron scattering on free atoms (He, Ne, and Ar).^{15,16} In this section we show results for e -Ar and e -Kr elastic scattering, and compare with results from use of the Hartree-Fock and the Hedin-Lundqvist potentials.

Differential cross sections (DCSs) in a.u.² as a function of scattering angle for elastic scattering at 300 and 500 eV and for different values of Δ are shown in Figs. 1 and 2 for Ar and in Fig. 3 for Kr. The solid lines show the results for $\Delta = 0$ eV, the dashed lines $\Delta = 20$ eV, and the dotted lines $\Delta = 40$ eV. Some experimental data and the result from the Hartree-Fock and the Hedin-Lundqvist approximations are also shown. The dependence on the parameter Δ is moderate. The best agreement for the present method is found with $\Delta = 40$ eV for Ar and with 0–20 eV for Kr. As shown in our

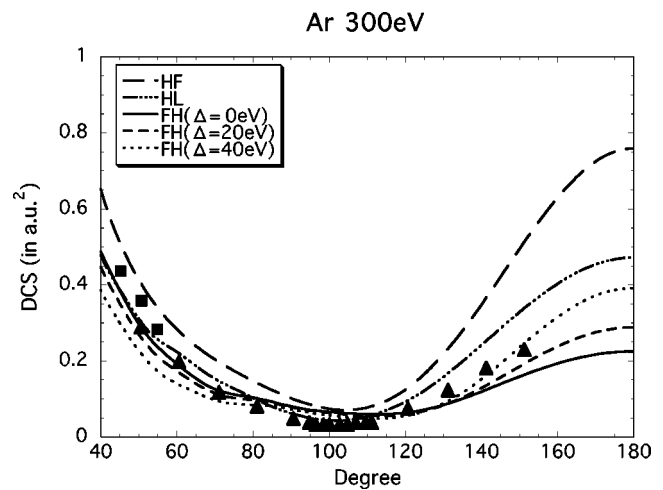


FIG. 2. Results for e -Ar scattering, but with a larger scattering angle ($\theta \geq 45^\circ$). The same notation as in Fig. 1.

earlier work, and as emphasized by Lee and Beni,²³ the largest contribution to the value of DCSs is due to nonlocal effects, of which the contribution from the optical potential is much larger than that from the HF exchange potential. With increasing energy the contribution from the optical po-

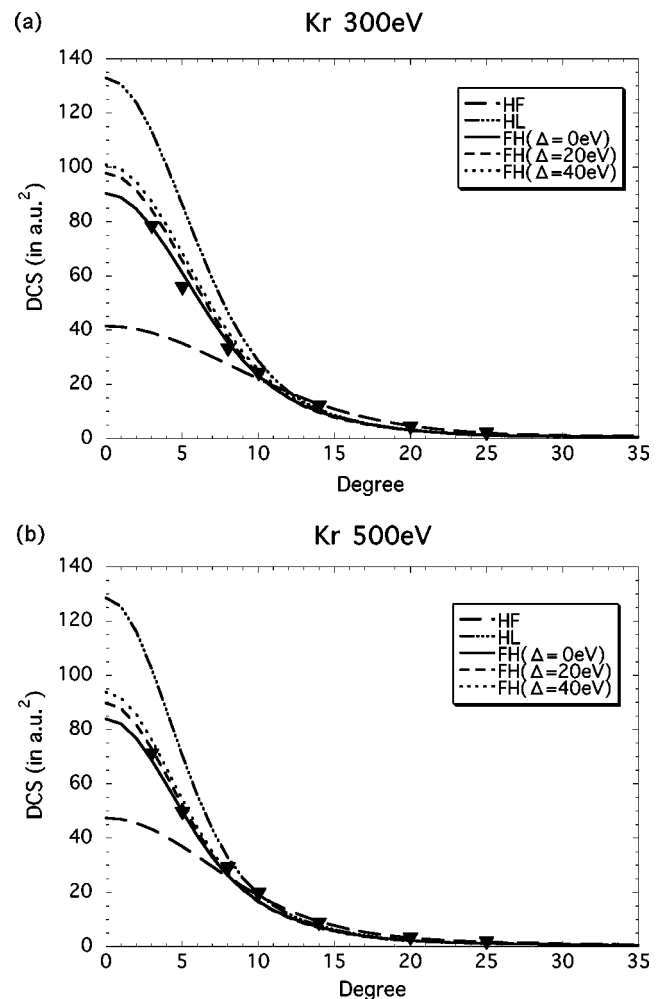


FIG. 3. Results for e -Kr scattering. The same notation as in Fig. 1. Experimental data \blacktriangledown are from Ref. 32.

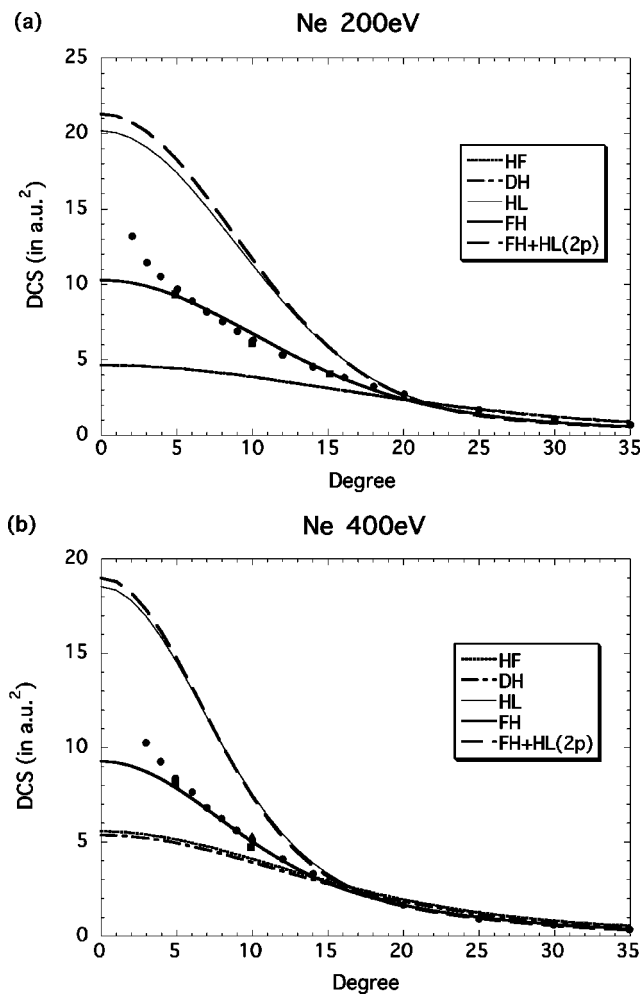


FIG. 4. The calculated elastic electron scattering cross sections from Ne at 200 eV (a) and 400 eV (b) for five different methods compared with experimental results. Two methods, Hartree-Fock (HF) and Dirac-Hara (DH), include only static effects, whereas the other three methods, Hedin-Lundqvist (HL), the present method (FH), and mixed FH+HL(2p) (see text), include dynamic effects.

tential tends to zero, and we can see that the difference between the FH and HF values diminishes when we go from 300 to 500 eV. The HL approximation, which is a local approximation for the FH potential, clearly does a poor job in representing the large nonlocal effects. The discrepancy even increases slightly with energy. The minimum in the experimental cross section at about $\theta=100^\circ$ is reproduced in all approximations, and the cross sections are correctly predicted to be small, but the percentage errors are large (Fig. 2). While the optical potential increases the HF DCS values for forward scattering, it decreases them for backscattering. The HL results are better for backscattering than for forward scattering.

In Figs. 4 and 5 we show results for Ne and Ar at 200 and 400 eV using different theories. We find that the local approximation of HF, the Dirac-Hara (DH) theory, agrees extremely well with the HF approximation. We further find that when we modify the FH method to treat the outermost shell with the HL approximation, the result comes very close to the HL approximation. This indicates, as expected, that the outermost shell dominates, and that the inner shells give very small contributions to the optical potential. Also for Ne, as

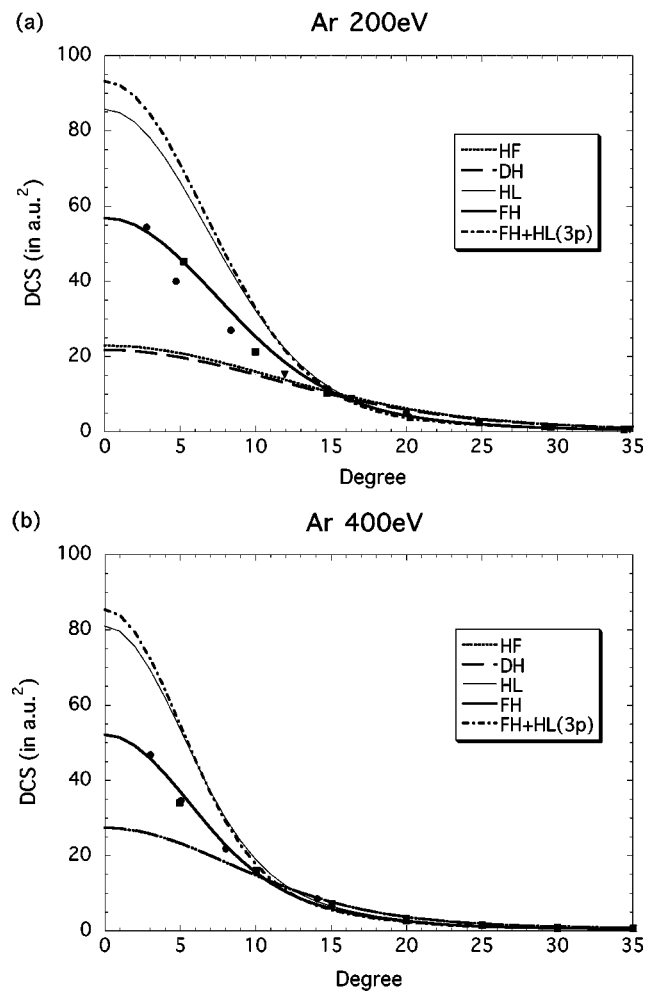


FIG. 5. Results for e -Ar scattering. The same notation as in Fig. 4.

for Ar and Kr, the full FH theory gives quite good results (with $\Delta=20$ eV). It should be noted that in the small-angle region the experimental results have large uncertainties since unscattered electrons easily come into the detector.

B. Elastic scattering from rare gas atoms in a solid

In solids the atoms are in close proximity of each other, which distorts their electronic structure from spherical symmetry. However, experience has shown that for many materials the situation can be simplified by using the muffin-tin approximation.¹ We then take the largest possible nonoverlapping spheres drawn about each nucleus, and use a spherically symmetric potential inside and a constant potential outside the muffin tins. Here we will only study muffin-tin potentials.

First we apply our optical potential theory to elastic scattering from Ne and Ar in their van der Waals solids. For these systems there is no G^0W^0 term in Eq. (2.3), whereas two-center terms such as the interatomic polarization term A_α^β given by Eq. (3.25) play some role. Another solid-state effect is the truncation when we construct the muffin-tin potential. Here we study these two effects on electron scattering from atoms in solids.

The truncation of the atomic region has influence on the convergence of the partial wave expansion. Figure 6 shows

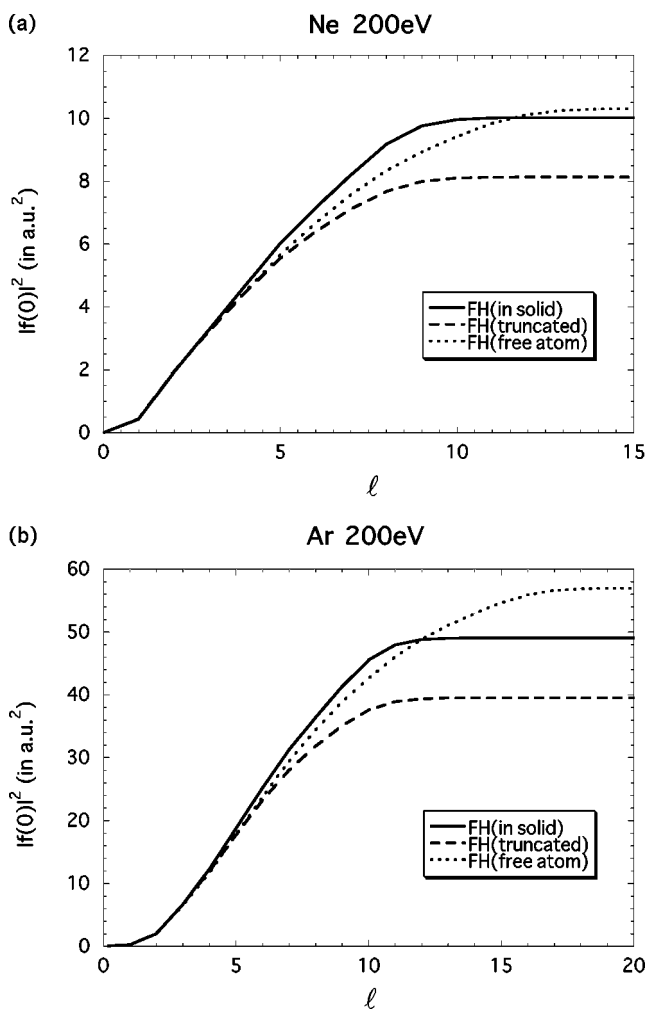


FIG. 6. Forward differential cross section in a.u. for electron elastic scattering from (a) Ne and (b) Ar in a solid state environment at 200 eV. The potential is truncated at the muffin-tin radius. The solid line (dashed line) is for a potential with (without) interatomic terms. The result for a free atom (dotted line) is shown for comparison.

the forward differential cross section in a.u.² for electron elastic scattering from (a) Ne and (b) Ar at 200 eV calculated by use of the nonlocal optical potential described in Sec. III. The convergence of the partial-wave expansion is investigated; the solid line (dashed line) is the result for *an atom in a solid* (*a truncated atom*). The result for a free atom (dotted line) is also shown for comparison. For *an atom in a solid*, the two-center terms in Eq. (3.25) are fully included, whereas they are neglected for *a truncated atom*. In both cases the atomic region is truncated at half the X - X distance ($X = \text{Ne, Ar}$). We thus use a different atomic radius than for a free atom; the boundary conditions at the radii give a set of phase shifts. For free atoms the charge density vanishes at a sufficiently large radius, whereas only inner core wave functions vanish at the muffin-tin radius, and outer core functions (say, $2p$ functions in Ne) still have finite values. As expected the convergence for *an atom in a solid* [$l_{\max} = 10(a), 12(b)$] is faster than for *a free atom* [$l_{\max} = 15(a), 18(b)$] because of the smaller atomic radius. In classical collision theory l_{\max} corresponds to an impact parameter; with a large atomic radius we have a large impact parameter. Both an *atom in a*

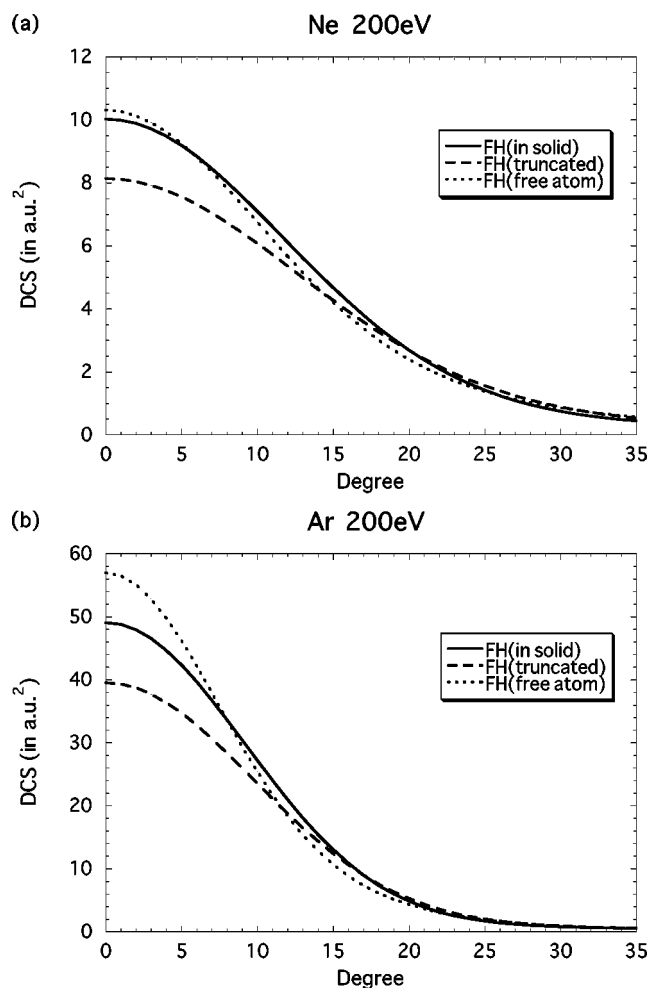


FIG. 7. The differential cross section in a.u. as a function of scattering angle for electron elastic scattering from Ne (a) and Ar (b) in a solid state environment at 200 eV. The same notation as in previous figure.

solid and a *truncated atom* give a converged $|f(0)|^2$ for nearly the same l_{\max} . The effect of the unscreened two-center terms in V^{pol} , given by the difference between FH (in solid) and FH (truncated) potentials, is quite large, but screening reduces the effect considerably. As a rough factor for this reduction we can take the square of the dielectric function, 1.8 for Ne and 3.8 for Ar. We then find that the interatomic coupling gives a smaller effect than that from truncation. As observed in the previous work, the long-range polarization part of the optical potential is also responsible for the slower convergence in comparison with the Hartree-Fock potential, where good convergence was found, $l_{\max} = 6$ (Ne) and $l_{\max} = 8$ (Ar).¹⁶

Figure 7 shows the differential cross section in a.u.² as a function of scattering angle for electron elastic scattering from Ne (a) and Ar (b) at 200 eV calculated by use of the present optical potential with the three different methods described above. The deviation between free atom and solid state (corrected for screening) scattering is usually largest for forward scattering. We note that even for van der Waals solids the solid-state effects (truncation plus screened interatomic contributions) are non-negligible.

In EXAFS the backscattering amplitudes play an important role. So far several calculations have been done based on

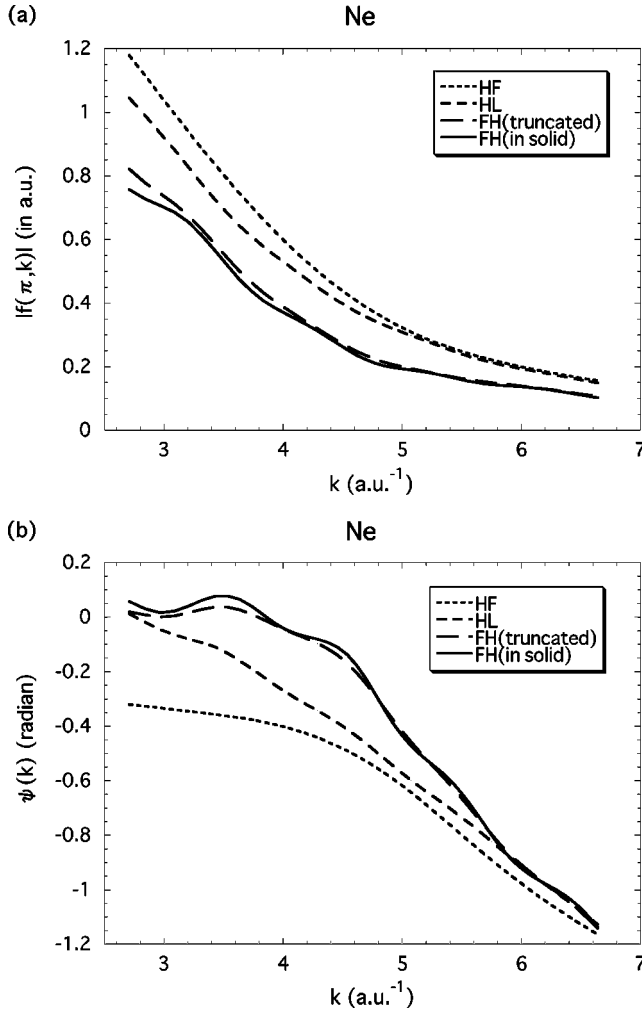


FIG. 8. The amplitude $|f(\pi, k)|$ (a), and the phase $\psi(k)$ (b) as functions of photoelectron wave vector k for solid Ne. Four different potentials are used: HF, HL, and FH with (FH in solid) and without interatomic terms (FH truncated).

the HL local density approximations for all electrons.^{23,27} The backscattering amplitude in the plane-wave approximation is written as

$$f(\pi, k) = |f(\pi, k)| \exp\{i\psi(k)\}. \quad (4.1)$$

Figure 8(a) shows $|f(\pi, k)|$ as a function of photoelectron wave vector k for a Ne atom in a solid Neon, and Fig. 8(b) shows the phase $\psi(k)$ for four different potentials, Hartree-Fock (HF), Hedin-Lundqvist (HL), and the present nonlocal optical potential with (FH in a solid) and without (FH truncated) interatomic effects. Figures 9(a) and 9(b) show similar results for e -Ar scattering. First we note that the interatomic effects are small for backscattering, and thus the *truncated atom* approximation is rather good for both $|f(\pi, k)|$ and $\psi(k)$. Further we see that when we go beyond the HF approximation, the factor $|f(\pi, k)|$ is substantially reduced as observed earlier.²³ The HL potential gives somewhat better results for $|f(\pi, k)|$ and $\psi(k)$ than the HF potential. All the optical potentials reduce the backscattering intensity while they increase the forward scattering. The nonlocal optical potentials give a weak oscillation in both $|f(\pi, k)|$ and $\psi(k)$, which may be due to the truncation or sharp cutoff at the

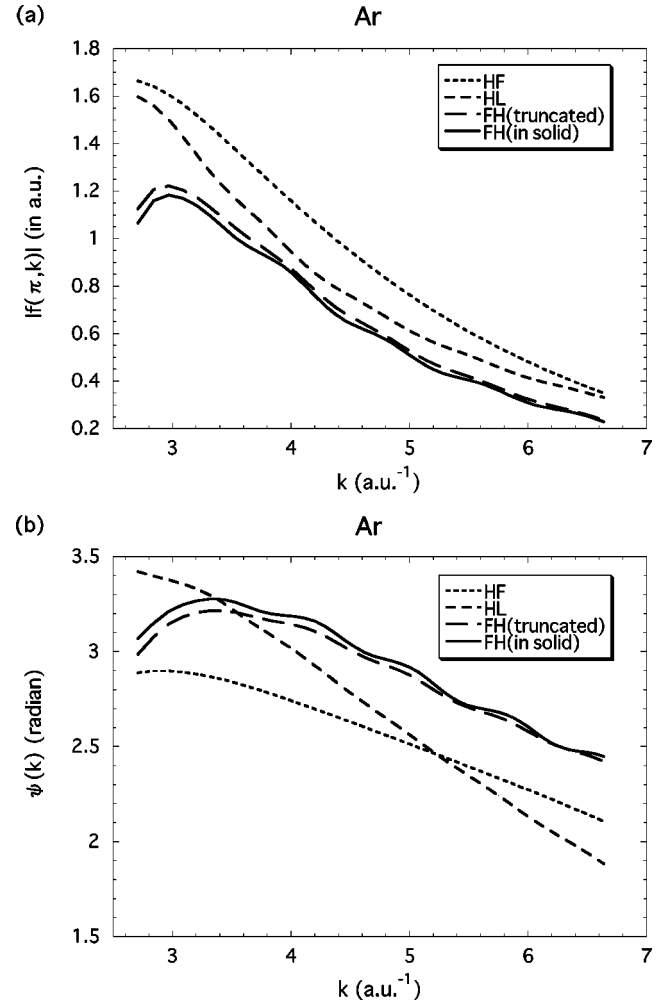


FIG. 9. The same quantities as in Fig. 8, but for solid Ar.

muffin-tin radius. In the case of Ar as compared with Ne the HL potential gives somewhat better results for the amplitude $|f(\pi, k)|$, while it gives somewhat worse results for the phase $\psi(k)$.

C. Elastic scattering from atoms in metals and semiconductors

We have studied five different potentials where we use the HF or HL potential for the ion core and the outer electrons ($3s^1 3p^3$ for Si, $3s^1$ for Na and $3d^{7.4} 4s^{0.6}$ for Fe), and where V^{pol} may be included or omitted. We use a notation, where, e.g., (HF,HL) means that the HF potential is used for core electrons and HL potential for outer electrons. The five potentials are HF=(HF,HF), HF+HL=(HF,HL), HL=(HL,HL), FH+HF=(HF,HF)+ V^{pol} , and FH=(HF,HL)+ V^{pol} . The case HF+HL was studied earlier by Echenique.²⁴

Figure 10 shows the differential cross section $|f(\theta)|^2$ as a function of scattering angle ($0^\circ \leq \theta \leq 35^\circ$) for electron scattering in Si (a), Na (b), and Fe (c) crystals at 200 eV. In the three upper curves we have an HL and in the two lower ones an HF potential for the outer electrons. It is clear that the choice of potential for the outer electrons is more important than that for the ion core. The importance of the ion core is related to how strongly bound the core electrons are. The minimum core excitation energy in Si, Fe, and Na, is respec-

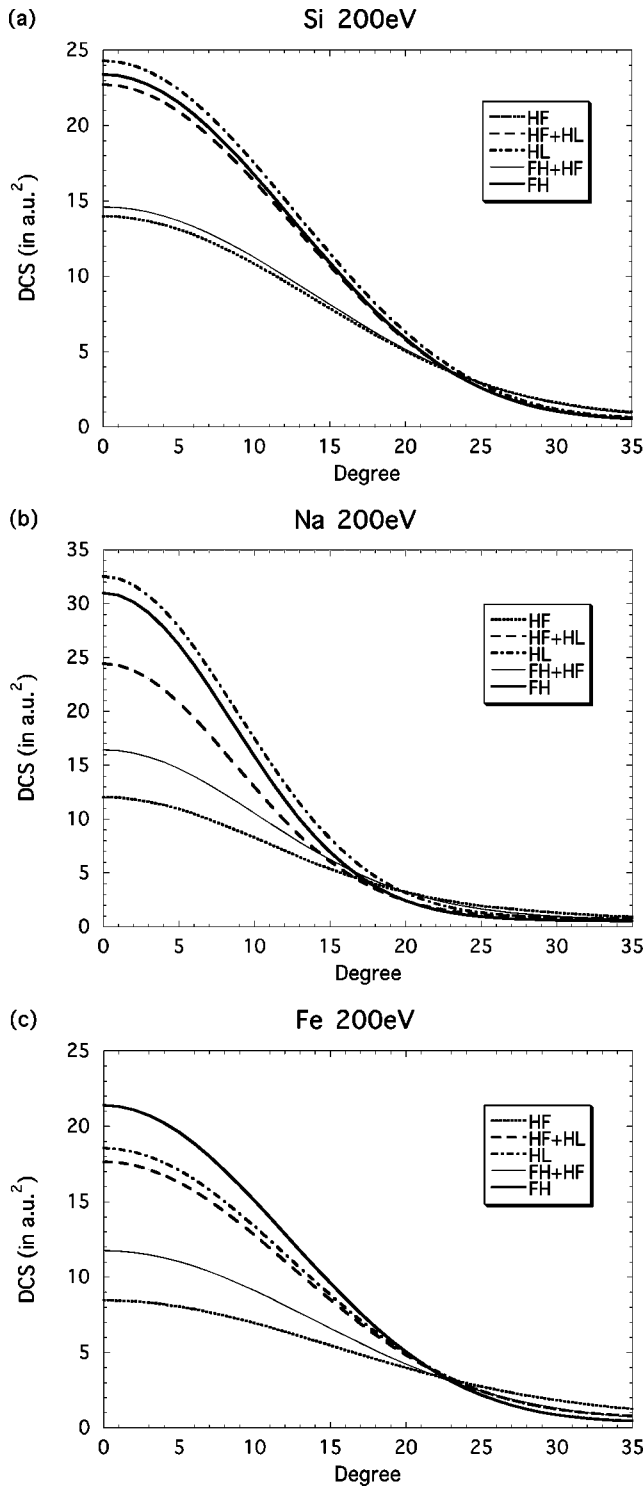


FIG. 10. The differential cross section $|f(\theta)|^2$ as function of the scattering angle for e -Si (a), e -Na (b), and e -Fe (c) at 200 eV. We used five different potentials (see text): HF=(HF,HF), HF+HL=(HF,HL), HL=(HL,HL), FH+HF=(HF,HF)+ V^{pol} , and FH=(HF,HL)+ V^{pol} .

tively, 100, 53, and 31 eV, which is reflected in the spread of the curves. We note that addition of V^{pol} has about the same effect irrespective of what potential is used for the outer electrons; i.e., the difference between the FH+HF and the HF curves is about the same as between the FH and the HF+HL curves. We also remark that the $3d$ electrons in Fe

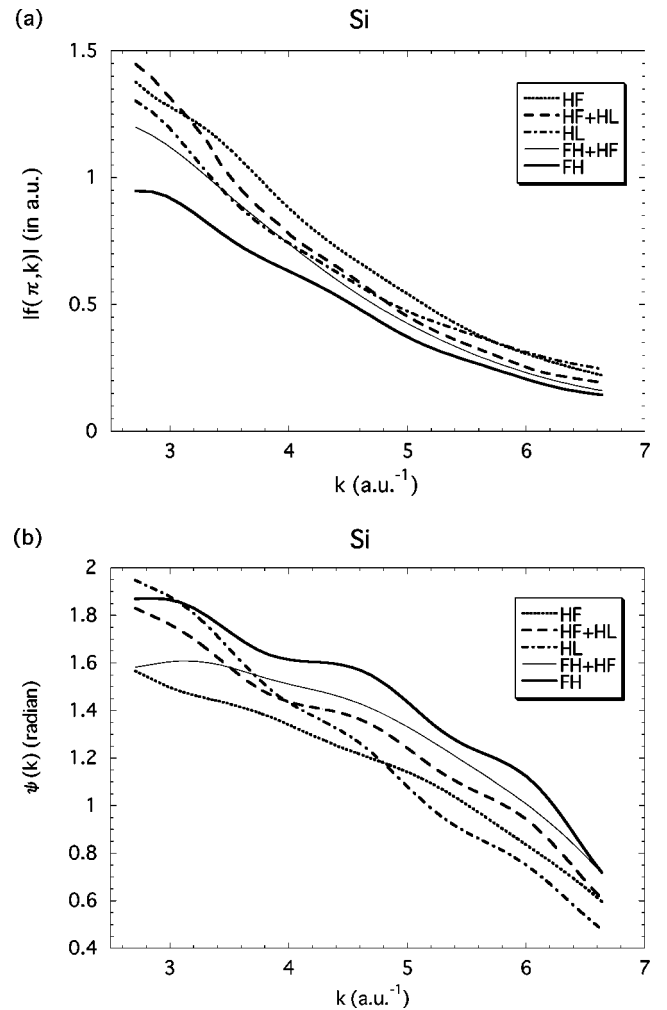


FIG. 11. The amplitude $|f(\pi, k)|$ (a), and the phase $\psi(k)$ (b) as functions of the photoelectron wave vector k for a Si crystal. The same five potentials as in Fig. 8 are used.

are treated by the local density approximation of the uniform electron gas self-energy, which is a rather rough approximation. A full treatment of the non-local $G^v W^v$ expression, however, leads to hard problems in finding a proper muffin-tin potential.

Next we study the backscattering amplitudes which are important in EXAFS analyses. Figures 11–13 show the amplitudes $|f(\pi, k)|$ and phases $\psi(k)$ for Si, Na, and Fe crystals as a function of k for the five different potentials discussed above. In comparison with the small-angle scattering shown in Fig. 10, the potential from the inner electrons is now more important. Thus we see that with increasing energy the FH=(HF,HL)+ V^{pol} and FH+HF=(HF,HF)+ V^{pol} curves approach each other, as do the HF=(HF,HF) and HF+HL=(HF,HL) curves. This result is expected; forward scattering corresponds to large impact parameters and dominance of the outer electrons, while backscattering corresponds to small impact parameters and a large influence also of the inner electrons. The fact that FH+HF and HF curves are separate at high energies shows that V^{pol} has an appreciable short-range part. Our result for Fe is a little different from that in the paper by Lee and Beni,²³ because they used a larger atomic radius.

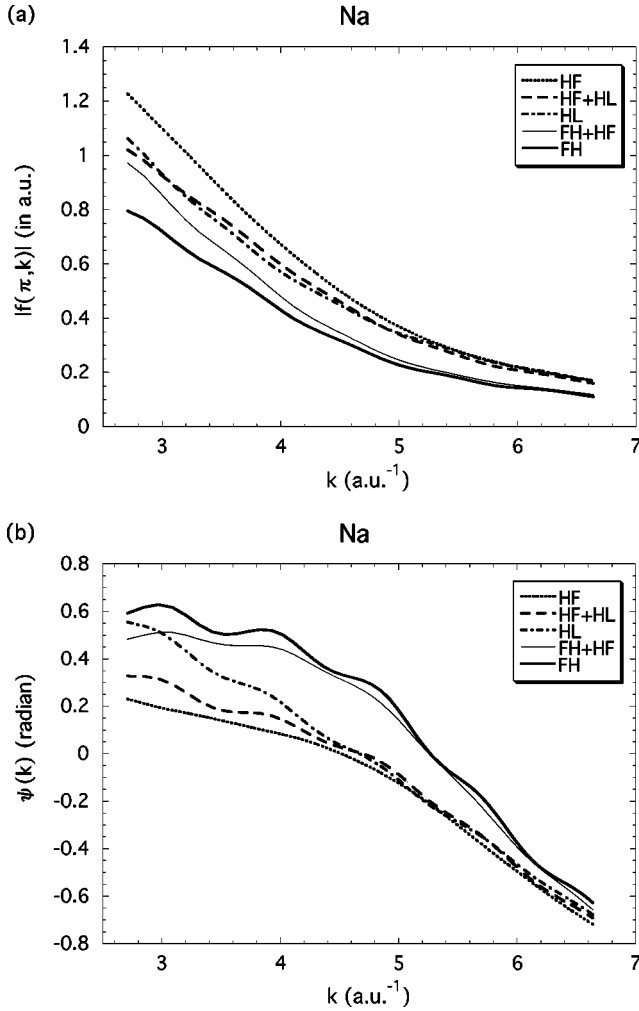


FIG. 12. The same as in Fig. 11, but for a Na metal.

The HL curves, which contrary to the other four cases have an HL and not an HF potential for the inner electrons, show no predictable behavior. This is not surprising since a local density electron gas expression cannot easily mimic a nonlocal rapidly varying ion core exchange potential. As pointed out in Ref. 21, Sec. 6, while in the inner of atoms the high electron density favors a local density description, the rapid variation of the charge density more than offsets this advantage.

V. CONCLUDING REMARKS

We have presented a theory for a crystal potential to be used in different electron spectroscopies like LEED, RHEED, XPS, XAFS, and EELFS at intermediate and high energies, say, above 50 eV. It is found that the core-polarization contribution V^{pol} to the potential plays an important role, not only for rare gas solids but also for metals like sodium and iron, whereas for silicon, with its very compact ion core, the effects are smaller.

In earlier work we studied V^{pol} for atoms. Here the theory is developed in more detail, and we also study muffin-tinned solid-state potentials. It is found that contributions to V^{pol} from unscreened interatomic couplings is appreciable, but that screening effects reduce these contributions to quite

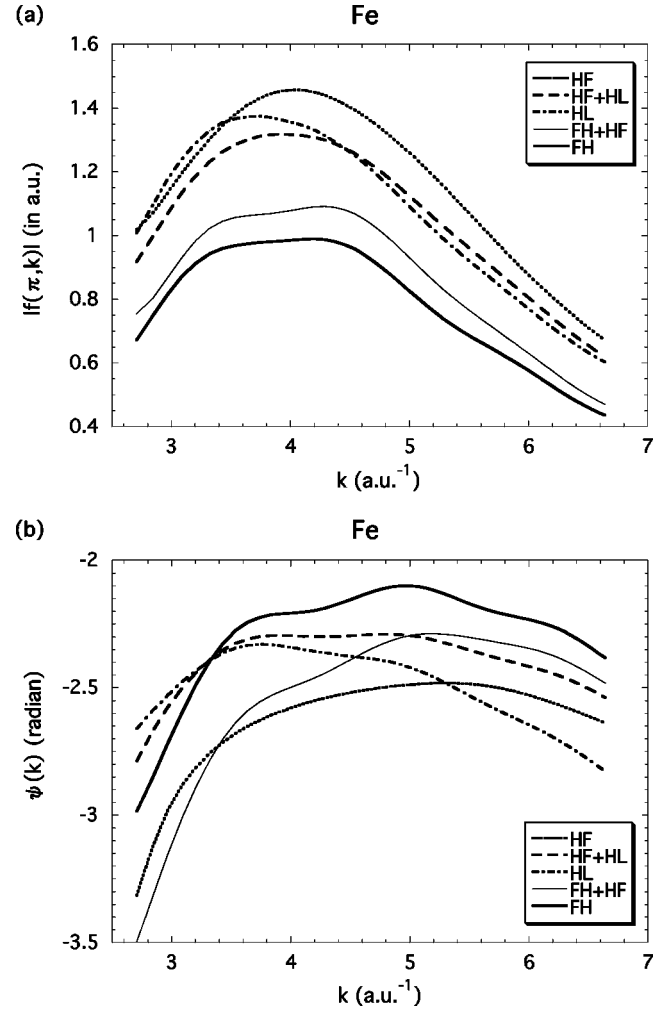


FIG. 13. The same as in Fig. 11, but for a Fe metal.

small values. The main uncertainties come from the choice of the effective excitation energy Δ and from the truncation of the nonlocal potential V^{pol} at the muffin-tin radius. The truncation effects are more serious for small scattering angles and less so for backscattering when the inner parts of the potential are important. The uncertainties in the forward scattering results are, however, of limited interest since forward scattering is anyhow usually difficult to observe.

Our equations should in principle be solved self-consistently. The self-consistency problem was studied in earlier papers,^{15,16} and a large effect was found for He but not for Ne. Also in the present calculations only small effects were obtained. The input data for the self-consistency were the Hartree solution for He and Hartree-Fock solution for Ne. For helium the Hartree solution is quite poor since there are just two electrons and exchange effects are comparatively large. If we instead take input data from HF or local density approximation (LDA) self-consistency effects are generally much smaller than those from the choice of Δ and from the truncations at the muffin-tin radius (for solids).

One point on which our theory should be improved is the handling of the optical potential from the outer electrons (valence and conduction electrons), $\Sigma^v = G^v W^v$. We have here used the Hedin-Lundqvist approximation which is based on electron gas properties. A full treatment of a nonlocal Σ^v

may, however, as for V^{pol} , meet difficulties in the muffin-tin process. Despite all the different limitations that we have discussed, we feel that our theory represents an important improvement on present ways to construct crystal potentials and that it adds to our understanding of the properties of the crystal potential.

ACKNOWLEDGMENTS

The authors are grateful to H. Tanaka and Dr. T. Konishi for their useful comments on this work, and to Dr. T. Yikegaki and A. Saito for their important contribution to this research project at an early stage.

- ¹J. B. Pendry, *Low Energy Electron Diffraction* (Academic Press, London, 1974).
- ²*Reflection High-Energy Electron Diffraction and Reflection Imaging of Surface States*, edited by P. K. Larsen and P. J. Dobson (Plenum Press, New York, 1988).
- ³C. S. Fadley, *Prog. Surf. Sci.* **16**, 275 (1985); in *Synchrotron Radiation Research, Advances in Surface Sciences*, edited by R. Z. Bachrach (Plenum Press, New York, 1990), Vol. 1, p. 421.
- ⁴E. A. Stern and S. M. Heald, in *Handbook on Synchrotron Radiation*, edited by E. E. Koch (North-Holland, Amsterdam, 1983), Vol. 1b, p. 955.
- ⁵M. DeCrescenzi, *CRC Crit. Rev. Solid State Mater. Sci.* **15**, 279 (1989).
- ⁶J. S. Bell and E. J. Squires, *Phys. Rev. Lett.* **3**, 96 (1959).
- ⁷L. Hedin, *Phys. Rev.* **139**, A796 (1965); *Ark. Fys.* **30**, 231 (1965).
- ⁸L. Hedin and S. Lundqvist, in *Solid State Physics*, edited by F. Seitz, D. Turnbull and H. Ehrenreich (Academic Press, New York, 1969), Vol. 23, p. 1.
- ⁹W. Bardyszewski and L. Hedin, *Phys. Scr.* **32**, 439 (1985).
- ¹⁰L. Hedin, *Physica B* **158**, 344 (1988).
- ¹¹T. Fujikawa and L. Hedin, *Phys. Rev. B* **40**, 11 507 (1989).
- ¹²T. Fujikawa, *J. Phys. Soc. Jpn.* **60**, 3904 (1991); *Surf. Sci.* **269/270**, 55 (1992).
- ¹³F. W. Byron and J. C. Joachain, *Phys. Rev. A* **9**, 2559 (1974); **15**, 128 (1977); *J. Phys. B* **10**, 207 (1977).
- ¹⁴T. Fujikawa, A. Saito, and L. Hedin, *Jpn. J. Appl. Phys., Suppl.* **32(S-2)**, 18 (1993).
- ¹⁵T. Fujikawa, T. Yikegaki, and L. Hedin, *J. Phys. Soc. Jpn.* **64**, 2351 (1995).
- ¹⁶T. Fujikawa, K. Hatada, T. Yikegaki and L. Hedin, *J. Electron Spectrosc. Relat. Phenom.* **88-91**, 649 (1998).
- ¹⁷J. C. Slater, *Phys. Rev.* **81**, 385 (1951).
- ¹⁸F. Herman, J. P. van Dyke, and I. B. Ortenburger, *Phys. Rev. Lett.* **22**, 807 (1969); R. Gáspár, *Acta Phys. Acad. Sci. Hung.* **3**, 263 (1954).
- ¹⁹P. A. Dirac, *Proc. Cambridge Philos. Soc.* **26**, 376 (1930).
- ²⁰S. Hara, *J. Phys. Soc. Jpn.* **22**, 710 (1967).
- ²¹L. Hedin and B. I. Lundqvist, *J. Phys. C* **4**, 2064 (1971).
- ²²L. J. Sham and W. Kohn, *Phys. Rev.* **145**, 561 (1966).
- ²³P. A. Lee and G. Beni, *Phys. Rev. B* **15**, 2862 (1977).
- ²⁴P. M. Echenique, *J. Phys. C* **9**, 3193 (1976).
- ²⁵P. M. Echenique and D. J. Titterton, *J. Phys. C* **10**, 625 (1977).
- ²⁶M. S. Woolfson, S. J. Gurman, and B. W. Holland, *Surf. Sci.* **117**, 450 (1982).
- ²⁷D. Lu and J. J. Rehr, *Phys. Rev. B* **37**, 6126 (1988).
- ²⁸R. Gunnella, M. Benfatto, A. Marcelli, and C. R. Natoli, *Solid State Commun.* **76**, 109 (1990).
- ²⁹J. Chaboy, *Solid State Commun.* **99**, 877 (1996).
- ³⁰M. Roy and S. J. Gurman, *J. Synchrotron Radiat.* **6**, 228 (1999).
- ³¹J. P. Bromberg, *J. Chem. Phys.* **61**, 963 (1974).
- ³²J. F. Williams and B. A. Wills, *J. Phys. B* **8**, 1670 (1975).
- ³³R. D. Du Bois and M. E. Rudd, *J. Phys. B* **8**, 1474 (1975).
- ³⁴R. H. Jansen, F. J. de Heer, H. J. Luyken, B. van Wingerden, and H. J. Blaauw, *J. Phys. B* **9**, 185 (1976).
- ³⁵T. Fujikawa and T. Miyanaga, *J. Phys. Soc. Jpn.* **62**, 4108 (1993).
- ³⁶J. J. Rehr, R. C. Albers, and S. I. Zabinsky, *Phys. Rev. Lett.* **69**, 3397 (1992).